Search for weakly decaying b -flavored pentaquarks

Aaij, R.; Adeva, B.; Adinolfi, M.; Ajaltouni, Z.; Akar, S.; Albrecht, J.; Alessio, F.; Alexander, M.; Alfonso Albero, A.; Ali, S.; Alkhazov, G.; Alvarez Cartelle, P.; Alves, A. A.; Amato, S.; Amerio, S.; Amhis, Y.; An, L.; Anderlini, L.; Andreassi, G.; Andreotti, M.

DOI:
10.1103/PhysRevD.97.032010

Document Version
Publisher's PDF, also known as Version of record

Search for weakly decaying b-flavored pentaquarks

R. Aaij *et al.*[*]
(LHCb Collaboration)

(Received 21 December 2017; published 16 February 2018; corrected 26 March 2018)

Investigations of the existence of pentaquark states containing a single b (anti)quark decaying weakly into four specific final states $J/\psi K^+\pi^- p$, $J/\psi K^-\pi^- p$, $J/\psi K^-\pi^+ p$, and $J/\psi\phi(1020)p$ are reported. The data sample corresponds to an integrated luminosity of 3.0 fb^{-1} in 7 and 8 TeV pp collisions acquired with the LHCb detector. Signals are not observed and upper limits are set on the product of the production cross section times branching fraction with respect to that of the Λ_b^0.

DOI: 10.1103/PhysRevD.97.032010

I. INTRODUCTION

The observation of charmonium pentaquark states with quark content $c\bar{c}uud$, by the LHCb [1] Collaboration in $\Lambda_b^0 \to J/\psi K^- p$ decays, raises many questions including: What is the internal structure of these pentaquarks? Do other pentaquark states exist? Are they molecular or tightly bound? In this analysis, we search for pentaquarks that contain a single b (anti)quark, that decay via the weak interaction. The Skyrme model [2] has been used to predict that the heavier the constituent quarks, the more tightly bound the pentaquark state [3–6]. This motivates our search for pentaquarks containing a b (anti)quark. No existing searches for weakly decaying pentaquarks containing a b (anti)quark have been published.

Consider the possible pentaquark states $\bar{b}duud$, $b\bar{u}udd$, $b\bar{d}uud$ and $\bar{b}suud$. We label these states as $P^+_{B^0p}$, $P^-_{\Lambda_b^0\pi^-}$, $P^+_{\Lambda_b^0\pi^+}$ and $P^+_{B_s^0p}$, respectively, where the subscript indicates the final states the pentaquark would predominantly decay into if it had sufficient mass to decay strongly into those states. While there are many possible decay modes of these states, we focus on modes containing a J/ψ meson in the final state because these candidates generally have relatively large efficiencies and reduced backgrounds in the LHCb experiment. The Feynman diagrams for the decay of the $P^+_{B^0p}$ and $P^+_{B_s^0p}$ states are shown in Fig. 1. The corresponding diagrams for the decay of $P^-_{\Lambda_b^0\pi^-}$ and $P^+_{\Lambda_b^0\pi^+}$ are similar to that shown in Fig. 1(a), with the decay of the state being driven by the $b \to c\bar{c}s$ transition. We reconstruct the $\phi(1020)$ meson[1] in the K^+K^- decay mode. We note that the $P^+_{B^0p}$ pentaquark might have some decays inhibited by Bose statistics if its structure is based on two identical ud diquarks, i.e. $\bar{b}(ud)(ud)$. Although the $P^+_{B_s^0p}$ state is expected to be produced at a smaller rate on the grounds that B_s^0 production in the LHCb experiment acceptance is only about 13% of the rate of the sum of B^+ and B^0 production [7], it would not have two identical diquarks, and hence none of its decays would suffer from spin-statistics suppression.

Table I lists all of the pentaquarks we search for along with their respective weak decay modes.[2] It is possible for these pentaquarks (P_B) to decay either strongly or weakly depending on their masses. The threshold mass for strong decay for $P^+_{B^0p}$ would be $m(B^0)+m(p)$, for $P^-_{\Lambda_b^0\pi^-}$ $m(\Lambda_b^0)+m(\pi^-)$, for $P^+_{\Lambda_b^0\pi^+}$ $m(\Lambda_b^0)+m(\pi^+)$ and for $P^+_{B_s^0p}$ $m(B_s^0)+m(p)$. Therefore, we define our signal search windows to be below these thresholds. Note that a fifth state, the $b\bar{s}uud$ pentaquark ($P^+_{\bar{B}_s^0p}$) could also decay into $J/\psi\phi p$, and thus is implicitly included in our searches. Should a signal be detected for mode *IV*, we would need to examine noncharmonium modes to distinguish between the possibilities.

II. DETECTOR DESCRIPTION AND DATA SAMPLES

The LHCb detector [8,9] is a single-arm forward spectrometer covering the pseudorapidity range $2<\eta<5$, designed for the study of particles containing b or c quarks. The detector includes a high-precision tracking system consisting of a silicon-strip vertex detector surrounding the

[*]Full author list given at the end of the article.

[1]Hereafter ϕ refers to the $\phi(1020)$ meson.

[2]Unless explicitly stated, mention of a particular mode implies the use of the charge-conjugated mode as well.

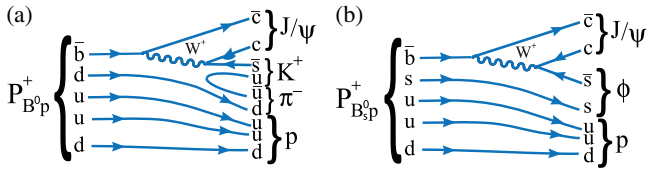

FIG. 1. Leading-order diagrams for pentaquark decay modes into (a) $J/\psi K^+\pi^- p$ or (b) $J/\psi\phi p$ final states.

pp interaction region, a large-area silicon-strip detector located upstream of a dipole magnet with a bending power of about 4 Tm, and three stations of silicon-strip detectors and straw drift tubes placed downstream of the magnet. The tracking system provides a measurement of momentum, p, of charged particles with a relative uncertainty that varies from 0.5% at low momentum to 1.0% at 200 GeV. The minimum distance of a track to a primary pp interaction vertex (PV), the impact parameter (IP), is measured with a resolution of $(15 + 29/p_{\mathrm{T}})$ μm, where p_{T} is the component of the momentum transverse to the beam, in GeV. Different types of charged hadrons are distinguished using information from two ring-imaging Cherenkov detectors (RICH). Photons, electrons and hadrons are identified by a calorimeter system consisting of scintillating-pad and preshower detectors, an electromagnetic calorimeter and a hadronic calorimeter. Muons are identified by a system composed of alternating layers of iron and multiwire proportional chambers.

The online event selection is performed by a trigger, which consists of a hardware stage, based on information from the calorimeter and muon systems, followed by a software stage, which applies a full event reconstruction. The subsequent software trigger is composed of two stages, the first of which performs a partial reconstruction and requires either a pair of well-reconstructed, oppositely charged muons having an invariant mass above 2.7 GeV, or a single well-reconstructed muon with high p_{T} and large IP. The second stage of the software trigger applies a full event reconstruction and, for this analysis, requires two opposite-sign muons to form a good-quality vertex that is well separated from all of the PVs, and to have an invariant mass within ± 120 MeV of the known J/ψ mass [10]. The data sample corresponds to 1.0 fb^{-1} of integrated luminosity collected with the LHCb detector in 7 TeV pp collisions and 2.0 fb^{-1} in 8 TeV collisions.

TABLE I. Quark content of the b-flavored pentaquarks and their weak decay modes explored here. We consider only the quark decay process $b \to c\bar{c}s$. The lower and upper bounds of the mass region searched are also given. (In this paper we use natural units where $\hbar = c = 1$.)

Mode	Quark content	Decay mode	Search window
I	$\bar{b}duud$	$P^+_{B^0 p} \to J/\psi K^+\pi^- p$	4668–6220 MeV
II	$b\bar{u}udd$	$P^-_{\Lambda_b^0\pi^-} \to J/\psi K^-\pi^- p$	4668–5760 MeV
III	$b\bar{d}uud$	$P^+_{\Lambda_b^0\pi^+} \to J/\psi K^-\pi^+ p$	4668–5760 MeV
IV	$\bar{b}suud$	$P^+_{B_s^0 p} \to J/\psi\phi p$	5055–6305 MeV

Simulated events are generated in the LHCb acceptance using PYTHIA [11], with a special LHCb parameter tune [12]. Pentaquark candidate (P_B) decays are generated uniformly in phase space. Decays of other hadronic particles are described by EVTGEN [13], in which final-state radiation is generated using PHOTOS [14]. The interaction of the generated particles with the detector, and its response, are implemented using the GEANT4 toolkit [15] as described in Ref. [16]. The lifetime of the simulated pentaquarks is set to 1.5 ps, consistent with that of most weakly decaying b hadrons [10].

III. EVENT SELECTION AND *B*-HADRON RECONSTRUCTION

A pentaquark candidate is reconstructed by combining a $J/\psi \to \mu^+\mu^-$ candidate with a proton, kaon, and pion (or kaon for mode *IV*). Our analysis strategy consists of a preselection based on loose particle identification (PID) and the kinematics of the decay, followed by a more sophisticated multivariate selection (MVA) classifier based on a boosted decision tree (BDT) [17], which uses multiple input variables, accounts for the correlations and outputs a single discriminant. In order to avoid bias, the data in the signal search regions were not examined (blinded) until all the selection requirements were decided.

In the preselection, the J/ψ candidates are formed from two oppositely charged particles with p_{T} greater than 500 MeV, identified as muons and consistent with originating from a common vertex but inconsistent with originating from any PV. The invariant mass of the $\mu^+\mu^-$ pair is required to be within $[-48, +43]$ MeV of the known J/ψ mass [10], corresponding to a window of about ± 3 times the mass resolution. The asymmetry in the mass window is due to the radiative tail. Pion, kaon, and proton candidates are required to be positively identified in the RICH detector, but with loose requirements as the MVA includes particle identification criteria. Kaon and proton candidates are required to have momenta greater than 5 and 10 GeV, respectively, to avoid regions with suboptimal particle identification. Each track must have an IP χ^2 greater 9 than with respect to the closest PV, must have p_{T} greater than 250 MeV, and the scalar sum of the tracks p_{T} is required to be larger than 900 MeV. All of the tracks forming the pentaquark state are required to form a good vertex and have a significant detachment from the PV. We also require that the cosine of the angle between the vector from the PV to the P_B candidate vertex ($\vec{V}_{PV-P_B}$) and the P_B candidate momentum vector ($\vec{p}_{P_B}$) be greater than 0.999. The invariant mass of the pentaquark states is calculated by constraining the invariant mass of the dimuon pair to the known J/ψ mass, the muon tracks to originate from the J/ψ vertex and the vector sum of the momenta of the final state particles to point back to the PV.

We measure the product of the production cross section and branching fraction of these pentaquark states and normalize it to the analogous measurement [18] by the LHCb Collaboration for the Λ_b^0 baryon in the $\Lambda_b^0 \to J/\psi K^- p$ decay. To this end, we impose the same kinematic requirements on the P_B candidate as applied to the Λ_b^0 candidates in that analysis, namely $p_T < 20$ GeV and $2.0 < y < 4.5$, where $y = \frac{1}{2}\ln(\frac{E+p_z}{E-p_z})$ is the rapidity, E the energy and p_z the component of the momentum along the beam direction. After these preselections, the product of trigger and reconstruction efficiencies is around 2% for all the modes.

IV. SELECTION OPTIMIZATION BY A MULTIVARIATE CLASSIFIER

The MVA classifier is trained using the simulated signal samples described at the end of Sec. II and a background sample of candidates in data with invariant masses within 0.5 GeV above the strong-decay threshold in each final state (see Fig. 2). We use 3×10^6 $P^+_{B^0 p} \to (J/\psi \to \mu^+\mu^-)K^+\pi^- p$ simulated events for modes I, II and III, with the $P^+_{B^0 p}$ mass set to 5750 MeV, and 3×10^6 $P^+_{B_s^0 p} \to (J/\psi \to \mu^+\mu^-)(\phi \to K^+K^-)p$ simulated events for mode IV, with the $P^+_{B_s^0 p}$ mass set to 5835 MeV. The dependence of the selection efficiency as a function of mass is accounted for in Sec. V.

The training samples needed to model the backgrounds in the signal regions must represent the actual backgrounds as closely as possible. Contamination in the background samples can occur from fully reconstructed weakly decaying b-hadrons that are combined with random particles. In mode I, we find contributions from $B^0 \to J/\psi K^+\pi^-$ decays and $B_s^0 \to J/\psi K^+K^-$ decays where one of the kaons is misidentified as a pion; then a random additional proton results in contamination in the background sample. In modes II and III, along with the B^0 and B_s^0 contaminations, a $\Lambda_b^0 \to J/\psi K^- p$ decay can be paired with a random pion. In mode IV, only the B^0 and B_s^0 contaminations are seen. These mistaken identification contributions in the background sample are found by looking at the invariant mass distributions obtained by switching one or more final-state particles to another mass hypothesis. If this produces a peak in the mass distribution at the mass of a known particle, we apply a veto in the background training sample eliminating all candidates within ± 12 MeV of the peaks, approximately $\pm 1.6\sigma$. No such peaks are seen in the signal region, after switching the mass hypotheses, for any of the modes. As an example, we show fully reconstructed decays in the background and signal regions for mode I in Fig. 3.

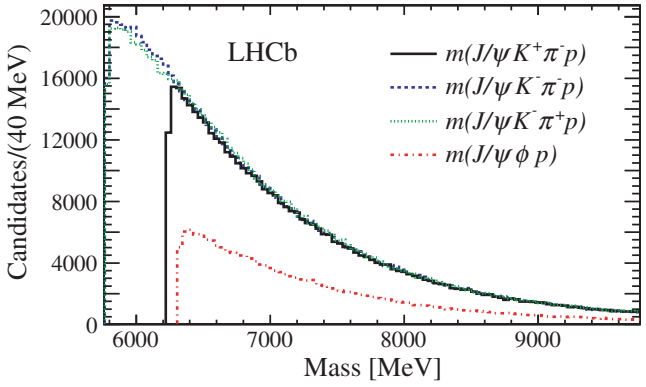

FIG. 2. Invariant mass distributions above the decay mass thresholds for the indicated modes.

The input variables used to train the classifier for modes I, II, and III are the same. We use the difference in the logarithm of the likelihood for two different particle hypotheses (DLL). They are the $\mathrm{DLL}(\mu - \pi)$ for the two muons, $\mathrm{DLL}(K - \pi)$ and $\mathrm{DLL}(K - p)$ for the kaon, $\mathrm{DLL}(p - \pi)$ and $\mathrm{DLL}(p - K)$ for the proton, and $\mathrm{DLL}(\pi - K)$ for the pion. Also used is the logarithm of χ^2_{IP}, defined as the difference in χ^2 of a given PV reconstructed with and without the considered K, π, and p tracks, and the χ^2 of the P_B to be consistent with originating from the PV. Other variables are the logarithm of the cosine of the angle of $\vec{p}_{P_B}$ with $\vec{V}_{PV-P_B}$, the flight distance of P_B, the scalar sum p_{T} of the K, π and p tracks, the χ^2/ndof of the fit of all the decay tracks to the P_B vertex, and of the two muon tracks to the J/ψ vertex with constraints that fix the dimuon invariant mass to the J/ψ mass and force the P_B candidate to point back to the PV, where ndof indicates the number of degrees of freedom. The input variables used to train the classifier for mode IV are similar, but with two kaons instead of a kaon and a pion.

Two important attributes of multivariate classifiers are signal efficiency and background rejection, both of which we wish to maximize. Using the input variables and training samples described earlier, we compared the performances of some common classifiers, including boosted decision trees (BDT), gradient boosted decision trees, linear discriminants, and likelihood estimators [19]. We base our MVA selection on the BDT algorithm. Once the BDT classifier is trained, it is evaluated by applying it to a separate testing sample (which is disjoint from the data sample used to train the classifier). The classifier assigns a response (called the BDT output) valued between–1 and 1 to the events, with background events tending toward low values and signal events to high values. These can be seen in Fig. 4(a) for mode I. The BDT outputs for other modes look very similar.

Discrimination between signal candidates, S, and background, B, is accomplished by choosing a BDT value that maximizes the metric $\frac{S}{a/2+\sqrt{B}}$, where a is the significance of the signal sought, which has the advantage of being independent of the signal cross section [20]. We choose a to be 3 for all modes, based on the assumption that we are

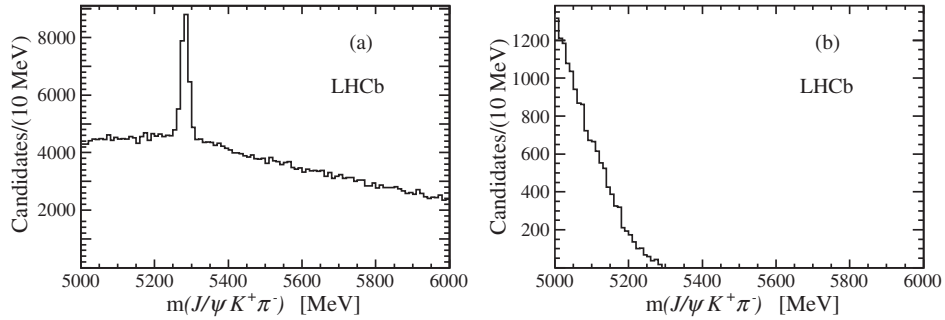

FIG. 3. For the $P^+_{B^0p} \to J/\psi K^+\pi^- p$ decay search (mode *I*), the invariant mass of $J/\psi K^+\pi^-$ combinations in the (a) region above threshold and in the (b) signal region. The peak in the sideband region results from B^0 decays.

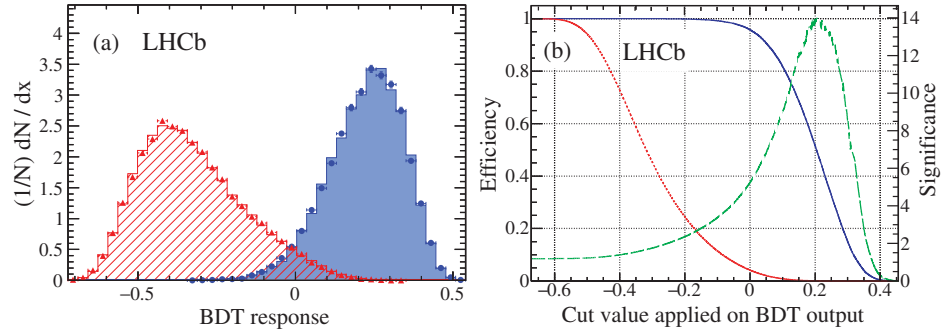

FIG. 4. (a) Outputs of the BDT classifier for the $J/\psi K^+\pi^- p$ final state. The circles (blue) show the signal training sample, and the triangles (red) show the background training sample, while the shaded (blue) histogram shows the signal test sample, and the diagonal (red) line-shaded histogram the background test sample. (b) Efficiencies of signal, solid (blue) curve, and background, dotted (red) curve, and the value of the $S/(\sqrt{B}+1.5)$, dashed (green) curve, called "significance," as a function of the BDT output.

in a situation of looking for a small signal in the midst of larger backgrounds. The variation of the signal and background efficiencies and the metric's value with the BDT output is shown in Fig. 4(b) for mode *I*. This variation of efficiencies and the metric with respect to the BDT value is similar for the other modes. After optimization, the BDT signal efficiency varies from 42.9% to 71.4% depending on the decay mode.

One cause of concern is reflections where the particle identification fails leading to the inclusion of other well-known final states. These are eliminated with a small loss of efficiency by removing candidate combinations within ± 12 MeV of the appropriate *b*-hadron mass. A list of these reflections in the particular modes of interest is given in Table II.

V. RESULTS

After the selections were decided upon, the analysis was unblinded. A search is conducted by scanning the P_B invariant mass distributions in the four final states shown in Fig. 5. The step size used in these scans is 4.0 MeV, corresponding to about half the invariant mass resolution. No signal is observed with the expected width of approximately 7.5 MeV. The P_B mass resolution seen in the simulated samples is 6.0 MeV for modes *I*, *II*, *III*, and 5.2 MeV for mode *IV* which, as expected, is similar to the 7.5 MeV width seen in data for the Λ_b^0 baryon in the $(J/\psi \to \mu^+\mu^-)K^- p$ final state, when the two muons are constrained to the J/ψ mass. In order to obtain conservative results, we set upper limits based on the wider 7.5 MeV signal width.

At each P_B scan mass value m_{P_B}, the signal region is a $\pm 2\sigma(m_{P_B})$ window around m_{P_B}, while the background is estimated by interpolating the yields in the sidebands starting at $3\sigma(m_{P_B})$ from m_{P_B} and extending to $5\sigma(m_{P_B})$, both below and above m_{P_B} following Ref. [21]. The statistical test at each mass is based on the profile likelihood ratio of Poisson-process hypotheses with and without a signal contribution, where the uncertainty on the background interpolation is modeled as purely Poisson (see Ref. [21] for details). No significant excess of signal candidates is observed over the expected background. The upper limits are set on the signal yields using the profile likelihood technique, in which systematic uncertainties are handled by including additional Gaussian terms in the likelihood.

In the absence of a significant signal, we set upper limits in each P_B candidate mass interval on the ratio

TABLE II. Decay modes that are vetoed for each pentaquark candidate mode and the specific particle misidentification that causes the reflection.

Search mode	Reflection	Particle misidentification
$P^+_{B^0p} \to J/\psi K^+\pi^- p$	$B^+ \to J/\psi K^+\pi^-\pi^+$	π^+ to p
	$B^+ \to J/\psi\pi^+\pi^- K^+$	π^+ to K^+ and K^+ to p
$P^-_{\Lambda_b^0\pi^-} \to J/\psi K^-\pi^- p$	$B^- \to J/\psi K^-\pi^-\pi^+$	π^+ to p
	$B^- \to J/\psi(\phi \to K^-K^+)\pi^-$	K^+ to p
$P^+_{\Lambda_b^0\pi^+} \to J/\psi K^-\pi^+ p$	$B^+ \to J/\psi(\phi \to K^-K^+)\pi^+$	K^+ to p
$P^+_{B_s^0 p} \to J/\psi\phi p$	$B^+ \to J/\psi\phi K^+$	K^+ to p

$$R = \frac{\sigma(pp \to P_B X)\cdot\mathcal{B}(P_B \to J/\psi X)}{\sigma(pp \to \Lambda_b^0 X)\cdot\mathcal{B}(\Lambda_b^0 \to J/\psi K^- p)}, \quad (1)$$

where we use the $\Lambda_b^0 \to J/\psi K^- p$ channel for normalization. The product of the production cross section and branching fraction of this channel has been measured by the LHCb Collaboration [18] to be

$$\begin{aligned}&\sigma(\Lambda_b^0, \sqrt{s} = 7\ \text{TeV})\cdot\mathcal{B}(\Lambda_b^0 \to J/\psi K^- p)\\ &\quad = 6.12 \pm 0.10 \pm 0.25\ \text{nb},\\ &\sigma(\Lambda_b^0, \sqrt{s} = 8\ \text{TeV})\cdot\mathcal{B}(\Lambda_b^0 \to J/\psi K^- p)\\ &\quad = 7.51 \pm 0.08 \pm 0.31\ \text{nb}, \end{aligned} \quad (2)$$

where the uncertainties are statistical and systematic, respectively. The systematic uncertainties include those on the luminosity and detection efficiencies that partially cancel, lowering the effective systematic uncertainty on the normalization. These measurements are averaged, taking into account the different luminosities at the two energies, to produce the overall normalization factor of $NF = 7.03 \pm 0.06 \pm 0.17$ nb.

Simulations have been generated at four different P_B masses for each decay mode. The total selection efficiency varies from 0.45% to 1.4% depending on mass and decay mode. The mass dependence of the efficiencies is parametrized by a second-order polynomial, for each decay mode, and incorporated into the upper limit calculation. The dominant source of uncertainty on the efficiency is systematic, and arises from the calibration applied to the particle identification as calculated by the simulation. This absolute efficiency uncertainty varies from 0.02% to 0.17% depending on the decay mode. The statistical uncertainties on the efficiency are negligible. Note that we are taking the P_B lifetime as 1.5 ps, and all simulated efficiencies assume that the P_B decays are given by phase space.

For modes *I*, *II*, and *III*, the upper limits on S are normalized to obtain the upper limits on R according to

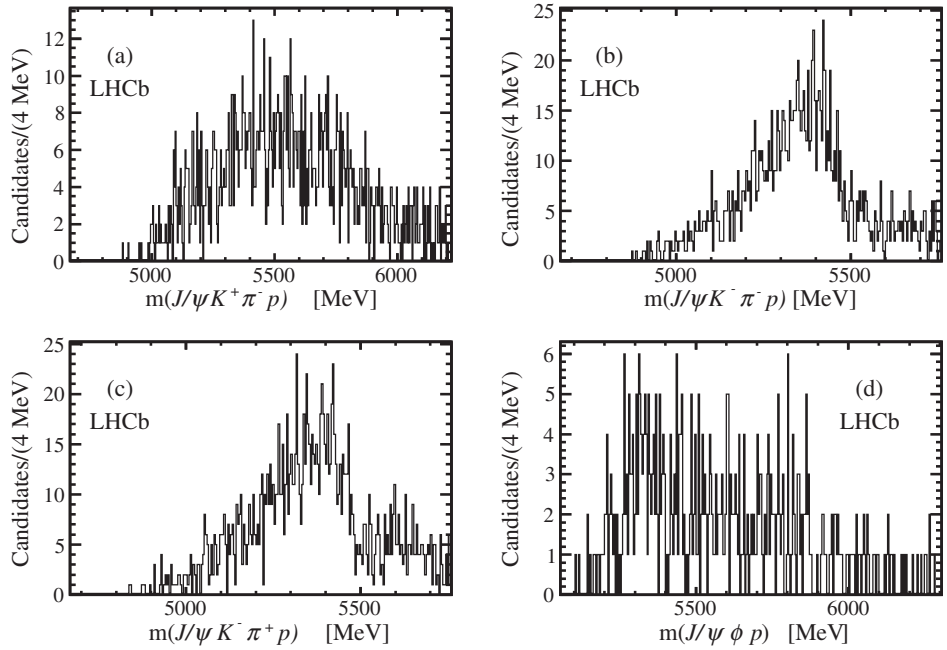

FIG. 5. Reconstructed mass distributions after the BDT selection for the (a) $J/\psi K^+\pi^- p$, (b) $J/\psi K^-\pi^- p$, (c) $J/\psi K^-\pi^+ p$, and (d) $J/\psi\phi p$ final states.

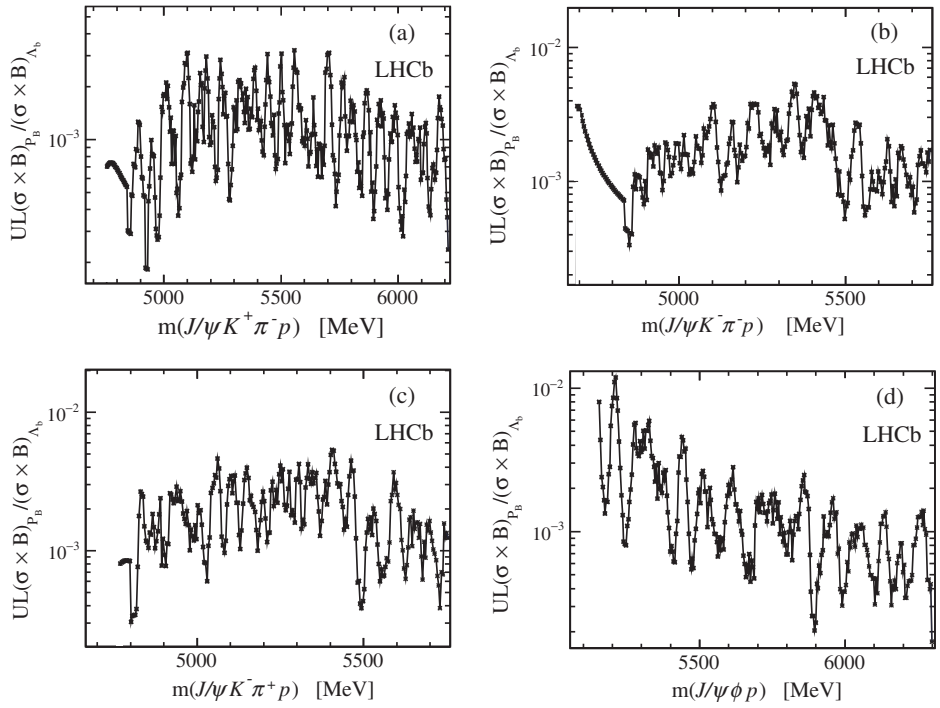

FIG. 6. Upper limits on R at 90% C.L. for (a) $J/\psi K^+\pi^- p$, (b) $J/\psi K^-\pi^- p$, (c) $J/\psi K^-\pi^+ p$, and (d) $J/\psi\phi p$ final states.

$$\mathrm{UL}(R) = \frac{\mathrm{UL}(S)}{\mathcal{L}\cdot\mathcal{B}(J/\psi\to\mu^+\mu^-)\cdot NF}, \tag{3}$$

where $\mathrm{UL}(S)$ is the efficiency corrected upper limit on S in each particular mass bin, $\mathcal{L}$ is the integrated luminosity and $\mathcal{B}(J/\psi\to\mu^+\mu^-)$ is the branching fraction for the $J/\psi\to\mu^+\mu^-$ decay. For mode *IV*, an additional factor of $\mathcal{B}(\phi\to K^+K^-)$, which is the branching fraction for the $\phi\to K^+K^-$ decay, is included in the denominator of Eq. (3).

The systematic uncertainty on $\mathrm{UL}(R)$ arises from the differences in analysis requirements between the search mode and the normalization mode (2%), which is estimated based on the differences the selection requirements could make in the relative efficiencies. The detection of an additional track (1%), given by the uncertainty in the data-driven tracking efficiency corrections, and the identification of this track (1%), given by the uncertainties in the particle identification calibration procedure, leads to an overall systematic uncertainty of 2.4%. For mode *IV*, the small uncertainty on $\mathcal{B}(\phi\to K^+K^-)$ is also taken into account. These uncertainties are added in quadrature with the uncertainty on NF. The upper limits on R are then increased linearly by this small systematic uncertainty. The results for $\mathrm{UL}(R)$ at 90% confidence level (C.L.) are shown in Fig. 6. Low invariant mass cutoffs in each mode are imposed when the efficiency uncertainty becomes large.

VI. CONCLUSIONS

We have searched for pentaquark states containing a b quark that decay weakly via the $b\to c\bar{c}s$ transition in the final states $J/\psi K^+\pi^- p$, $J/\psi K^-\pi^- p$, $J/\psi K^-\pi^+ p$, and $J/\psi\phi p$. Such states have been speculated to exist [3–6]. No evidence for these decays is found. Upper limits at 90% confidence level on the ratio of the production cross sections of these states times the branching fractions into the search modes, with respect to the production and decay of the Λ_b^0 baryon in the mode $J/\psi K^- p$ (R, see Eq. (1) are found to be about 10^{-3}, depending on the final state and the hypothesized mass of the pentaquark state.

ACKNOWLEDGMENTS

We thank I. Klebanov for useful discussions. We express our gratitude to our colleagues in the CERN accelerator departments for the excellent performance of the LHC. We thank the technical and administrative staff at the LHCb institutes. We acknowledge support from CERN and from the following national agencies: CAPES, CNPq, FAPERJ and FINEP (Brazil); MOST and NSFC (China); CNRS/IN2P3 (France); BMBF, DFG and MPG (Germany); INFN (Italy); NWO (The Netherlands); MNiSW and NCN (Poland); MEN/IFA (Romania); MinES and FASO (Russia); MinECo (Spain); SNSF and SER (Switzerland); NASU (Ukraine); STFC (United Kingdom); NSF (USA). We acknowledge the computing resources that are provided by CERN, IN2P3 (France), KIT and DESY (Germany), INFN (Italy), SURF (The

Netherlands), PIC (Spain), GridPP (United Kingdom), RRCKI and Yandex LLC (Russia), CSCS (Switzerland), IFIN-HH (Romania), CBPF (Brazil), PL-GRID (Poland) and OSC (USA). We are indebted to the communities behind the multiple open-source software packages on which we depend. Individual groups or members have received support from AvH Foundation (Germany), EPLANET, Marie Skłodowska-Curie Actions and ERC (European Union), ANR, Labex P2IO, ENIGMASS and OCEVU, and Région Auvergne-Rhône-Alpes (France), RFBR and Yandex LLC (Russia), GVA, XuntaGal and GENCAT (Spain), Herchel Smith Fund, the Royal Society, the English-Speaking Union and the Leverhulme Trust (United Kingdom).

[1] R. Aaij *et al.* (LHCb Collaboration), Observation of $J/\psi p$ Resonances Consistent with Pentaquark States in $\Lambda_b^0 \to J/\psi K^- p$ Decays, Phys. Rev. Lett. **115**, 072001 (2015).
[2] T. H. R. Skyrme, A non-linear field theory, Proc. R. Soc. A **260**, 127 (1961).
[3] I. Klebanov (private communication).
[4] I. W. Stewart, M. E. Wessling, and M. B. Wise, Stable heavy pentaquark states, Phys. Lett. B **590**, 185 (2004).
[5] A. K. Leibovich, Z. Ligeti, I. W. Stewart, and M. B. Wise, Predictions for nonleptonic Λ_b^0 and Θ_b decays, Phys. Lett. B **586**, 337 (2004).
[6] Y. S. Oh, B. Y. Park, and D. P. Min, Pentaquark exotic baryons in the Skyrme model, Phys. Lett. B **331**, 362 (1994).
[7] R. Aaij *et al.* (LHCb Collaboration), Measurement of b-hadron production fractions in 7 TeV pp collisions, Phys. Rev. D **85**, 032008 (2012).
[8] A. A. Alves Jr. *et al.* (LHCb Collaboration), The LHCb detector at the LHC, J. Instrum. **3**, S08005 (2008).
[9] R. Aaij *et al.* (LHCb Collaboration), LHCb detector performance, Int. J. Mod. Phys. A **30**, 1530022 (2015).
[10] C. Patrignani*et al.* (Particle Data Group), Review of particle physics, Chin. Phys. C **40**, 100001 (2016).
[11] T. Sjöstrand, S. Mrenna, and P. Skands, PYTHIA 6.4 physics and manual, J. High Energy Phys. 05 (2006) 026; A brief introduction to PYTHIA 8.1, Comput. Phys. Commun. **178**, 852 (2008).
[12] I. Belyaev *et al.*, Handling of the generation of primary events in Gauss, the LHCb simulation framework, J. Phys. Conf. Ser. **331**, 032047 (2011).
[13] D. J. Lange, The EvtGen particle decay simulation package, Nucl. Instrum. Methods Phys. Res., Sect. A **462**, 152 (2001).
[14] P. Golonka and Z. Was, PHOTOS Monte Carlo: A precision tool for QED corrections in Z and W decays, Eur. Phys. J. C **45**, 97 (2006).
[15] J. Allison *et al.* (Geant4 Collaboration), Geant4 developments and applications, IEEE Trans. Nucl. Sci. **53**, 270 (2006); S. Agostinelli *et al.* (Geant4 Collaboration), Geant4: A simulation toolkit, Nucl. Instrum. Methods Phys. Res., Sect. A **506**, 250 (2003).
[16] M. Clemencic, G. Corti, S. Easo, C. R. Jones, S. Miglioranzi, M. Pappagallo, and P. Robbe, The LHCb simulation application, Gauss: Design, evolution and experience, J. Phys. Conf. Ser. **331**, 032023 (2011).
[17] L. Breiman, J. H. Friedman, R. A. Olshen, and C. J. Stone, *Classification and Regression Trees* (Wadsworth International Group, Belmont, California, 1984).
[18] R. Aaij *et al.* (LHCb Collaboration), Study of the production of Λ_b^0 and $\bar{B}^0$ hadrons in pp collisions and first measurement of the $\Lambda_b^0 \to J/\psi p K^-$ branching fraction, Chin. Phys. C **40**, 011001 (2016).
[19] A. Hoecker *et al.*, TMVA: Toolkit for multivariate data analysis, *Proc. Sci.*, ACAT2007 (2007) 040 [arXiv:physics/0703039].
[20] G. Punzi, Sensitivity of searches for new signals and its optimization, in *Statistical Problems in Particle Physics, Astrophysics, and Cosmology*, edited by L. Lyons, R. Mount, and R. Reitmeyer (World Scientific, Singapore, 2003), p. 79.
[21] M. Williams, Searching for a particle of unknown mass and lifetime in the presence of an unknown non-monotonic background, J. Instrum. **10**, P06002 (2015).

Correction: The copyright statement contained an error and has been corrected.

R. Aaij,[40] B. Adeva,[39] M. Adinolfi,[48] Z. Ajaltouni,[5] S. Akar,[59] J. Albrecht,[10] F. Alessio,[40] M. Alexander,[53] A. Alfonso Albero,[38] S. Ali,[43] G. Alkhazov,[31] P. Alvarez Cartelle,[55] A. A. Alves Jr.,[59] S. Amato,[2] S. Amerio,[23] Y. Amhis,[7] L. An,[3] L. Anderlini,[18] G. Andreassi,[41] M. Andreotti,[17,a] J. E. Andrews,[60] R. B. Appleby,[56] F. Archilli,[43] P. d'Argent,[12] J. Arnau Romeu,[6] A. Artamonov,[37] M. Artuso,[61] E. Aslanides,[6] M. Atzeni,[42] G. Auriemma,[26] M. Baalouch,[5] I. Babuschkin,[56] S. Bachmann,[12] J. J. Back,[50] A. Badalov,[38,b] C. Baesso,[62] S. Baker,[55] V. Balagura,[7,c] W. Baldini,[17] A. Baranov,[35] R. J. Barlow,[56] C. Barschel,[40] S. Barsuk,[7] W. Barter,[56] F. Baryshnikov,[32] V. Batozskaya,[29] V. Battista,[41]

A. Bay,[41] L. Beaucourt,[4] J. Beddow,[53] F. Bedeschi,[24] I. Bediaga,[1] A. Beiter,[61] L. J. Bel,[43] N. Beliy,[63] V. Bellee,[41] N. Belloli,[21,d] K. Belous,[37] I. Belyaev,[32,40] E. Ben-Haim,[8] G. Bencivenni,[19] S. Benson,[43] S. Beranek,[9] A. Berezhnoy,[33] R. Bernet,[42] D. Berninghoff,[12] E. Bertholet,[8] A. Bertolin,[23] C. Betancourt,[42] F. Betti,[15] M. O. Bettler,[40] M. van Beuzekom,[43] Ia. Bezshyiko,[42] S. Bifani,[47] P. Billoir,[8] A. Birnkraut,[10] A. Bizzeti,[18,e] M. Bjørn,[57] T. Blake,[50] F. Blanc,[41] S. Blusk,[61] V. Bocci,[26] T. Boettcher,[58] A. Bondar,[36,f] N. Bondar,[31] I. Bordyuzhin,[32] S. Borghi,[56,40] M. Borisyak,[35] M. Borsato,[39] F. Bossu,[7] M. Boubdir,[9] T. J. V. Bowcock,[54] E. Bowen,[42] C. Bozzi,[17,40] S. Braun,[12] J. Brodzicka,[27] D. Brundu,[16] E. Buchanan,[48] C. Burr,[56] A. Bursche,[16,g] J. Buytaert,[40] W. Byczynski,[40] S. Cadeddu,[16] H. Cai,[64] R. Calabrese,[17,a] R. Calladine,[47] M. Calvi,[21,d] M. Calvo Gomez,[38,b] A. Camboni,[38,b] P. Campana,[19] D. H. Campora Perez,[40] L. Capriotti,[56] A. Carbone,[15,h] G. Carboni,[25,i] R. Cardinale,[20,j] A. Cardini,[16] P. Carniti,[21,d] L. Carson,[52] K. Carvalho Akiba,[2] G. Casse,[54] L. Cassina,[21] M. Cattaneo,[40] G. Cavallero,[20,40,j] R. Cenci,[24,k] D. Chamont,[7] M. G. Chapman,[48] M. Charles,[8] Ph. Charpentier,[40] G. Chatzikonstantinidis,[47] M. Chefdeville,[4] S. Chen,[16] S. F. Cheung,[57] S.-G. Chitic,[40] V. Chobanova,[39] M. Chrzaszcz,[42] A. Chubykin,[31] P. Ciambrone,[19] X. Cid Vidal,[39] G. Ciezarek,[40] P. E. L. Clarke,[52] M. Clemencic,[40] H. V. Cliff,[49] J. Closier,[40] V. Coco,[40] J. Cogan,[6] E. Cogneras,[5] V. Cogoni,[16,g] L. Cojocariu,[30] P. Collins,[40] T. Colombo,[40] A. Comerma-Montells,[12] A. Contu,[16] G. Coombs,[40] S. Coquereau,[38] G. Corti,[40] M. Corvo,[17,a] C. M. Costa Sobral,[50] B. Couturier,[40] G. A. Cowan,[52] D. C. Craik,[58] A. Crocombe,[50] M. Cruz Torres,[1] R. Currie,[52] C. D'Ambrosio,[40] F. Da Cunha Marinho,[2] C. L. Da Silva,[73] E. Dall'Occo,[43] J. Dalseno,[48] A. Davis,[3] O. De Aguiar Francisco,[40] K. De Bruyn,[40] S. De Capua,[56] M. De Cian,[12] J. M. De Miranda,[1] L. De Paula,[2] M. De Serio,[14,l] P. De Simone,[19] C. T. Dean,[53] D. Decamp,[4] L. Del Buono,[8] H.-P. Dembinski,[11] M. Demmer,[10] A. Dendek,[28] D. Derkach,[35] O. Deschamps,[5] F. Dettori,[54] B. Dey,[65] A. Di Canto,[40] P. Di Nezza,[19] H. Dijkstra,[40] F. Dordei,[40] M. Dorigo,[40] A. Dosil Suárez,[39] L. Douglas,[53] A. Dovbnya,[45] K. Dreimanis,[54] L. Dufour,[43] G. Dujany,[8] P. Durante,[40] J. M. Durham,[73] D. Dutta,[56] R. Dzhelyadin,[37] M. Dziewiecki,[12] A. Dziurda,[40] A. Dzyuba,[31] S. Easo,[51] M. Ebert,[52] U. Egede,[55] V. Egorychev,[32] S. Eidelman,[36,f] S. Eisenhardt,[52] U. Eitschberger,[10] R. Ekelhof,[10] L. Eklund,[53] S. Ely,[61] S. Esen,[12] H. M. Evans,[49] T. Evans,[57] A. Falabella,[15] N. Farley,[47] S. Farry,[54] D. Fazzini,[21,d] L. Federici,[25] D. Ferguson,[52] G. Fernandez,[38] P. Fernandez Declara,[40] A. Fernandez Prieto,[39] F. Ferrari,[15] L. Ferreira Lopes,[41] F. Ferreira Rodrigues,[2] M. Ferro-Luzzi,[40] S. Filippov,[34] R. A. Fini,[14] M. Fiorini,[17,a] M. Firlej,[28] C. Fitzpatrick,[41] T. Fiutowski,[28] F. Fleuret,[7,c] M. Fontana,[16,40] F. Fontanelli,[20,j] R. Forty,[40] V. Franco Lima,[54] M. Frank,[40] C. Frei,[40] J. Fu,[22,m] W. Funk,[40] E. Furfaro,[25,i] C. Färber,[40] E. Gabriel,[52] A. Gallas Torreira,[39] D. Galli,[15,h] S. Gallorini,[23] S. Gambetta,[52] M. Gandelman,[2] P. Gandini,[22] Y. Gao,[3] L. M. Garcia Martin,[71] J. García Pardiñas,[39] J. Garra Tico,[49] L. Garrido,[38] D. Gascon,[38] C. Gaspar,[40] L. Gavardi,[10] G. Gazzoni,[5] D. Gerick,[12] E. Gersabeck,[56] M. Gersabeck,[56] T. Gershon,[50] Ph. Ghez,[4] S. Gianì,[41] V. Gibson,[49] O. G. Girard,[41] L. Giubega,[30] K. Gizdov,[52] V. V. Gligorov,[8] D. Golubkov,[32] A. Golutvin,[55,69,n] A. Gomes,[1,o] I. V. Gorelov,[33] C. Gotti,[21,d] E. Govorkova,[43] J. P. Grabowski,[12] R. Graciani Diaz,[38] L. A. Granado Cardoso,[40] E. Graugés,[38] E. Graverini,[42] G. Graziani,[18] A. Grecu,[30] R. Greim,[9] P. Griffith,[16] L. Grillo,[56] L. Gruber,[40] B. R. Gruberg Cazon,[57] O. Grünberg,[67] E. Gushchin,[34] Yu. Guz,[37] T. Gys,[40] C. Göbel,[62] T. Hadavizadeh,[57] C. Hadjivasiliou,[5] G. Haefeli,[41] C. Haen,[40] S. C. Haines,[49] B. Hamilton,[60] X. Han,[12] T. H. Hancock,[57] S. Hansmann-Menzemer,[12] N. Harnew,[57] S. T. Harnew,[48] C. Hasse,[40] M. Hatch,[40] J. He,[63] M. Hecker,[55] K. Heinicke,[10] A. Heister,[9] K. Hennessy,[54] P. Henrard,[5] L. Henry,[71] E. van Herwijnen,[40] M. Heß,[67] A. Hicheur,[2] D. Hill,[57] P. H. Hopchev,[41] W. Hu,[65] W. Huang,[63] Z. C. Huard,[59] W. Hulsbergen,[43] T. Humair,[55] M. Hushchyn,[35] D. Hutchcroft,[54] P. Ibis,[10] M. Idzik,[28] P. Ilten,[47] R. Jacobsson,[40] J. Jalocha,[57] E. Jans,[43] A. Jawahery,[60] F. Jiang,[3] M. John,[57] D. Johnson,[40] C. R. Jones,[49] C. Joram,[40] B. Jost,[40] N. Jurik,[57] S. Kandybei,[45] M. Karacson,[40] J. M. Kariuki,[48] S. Karodia,[53] N. Kazeev,[35] M. Kecke,[12] F. Keizer,[49] M. Kelsey,[61] M. Kenzie,[49] T. Ketel,[44] E. Khairullin,[35] B. Khanji,[12] C. Khurewathanakul,[41] T. Kirn,[9] S. Klaver,[19] K. Klimaszewski,[29] T. Klimkovich,[11] S. Koliiev,[46] M. Kolpin,[12] R. Kopecna,[12] P. Koppenburg,[43] A. Kosmyntseva,[32] S. Kotriakhova,[31] M. Kozeiha,[5] L. Kravchuk,[34] M. Kreps,[50] F. Kress,[55] P. Krokovny,[36,f] W. Krzemien,[29] W. Kucewicz,[27,p] M. Kucharczyk,[27] V. Kudryavtsev,[36,f] A. K. Kuonen,[41] T. Kvaratskheliya,[32,40] D. Lacarrere,[40] G. Lafferty,[56] A. Lai,[16] G. Lanfranchi,[19] C. Langenbruch,[9] T. Latham,[50] C. Lazzeroni,[47] R. Le Gac,[6] A. Leflat,[33,40] J. Lefrançois,[7] R. Lefèvre,[5] F. Lemaitre,[40] E. Lemos Cid,[39] O. Leroy,[6] T. Lesiak,[27] B. Leverington,[12] P.-R. Li,[63] T. Li,[3] Y. Li,[7] Z. Li,[61] X. Liang,[61] T. Likhomanenko,[68] R. Lindner,[40] F. Lionetto,[42] V. Lisovskyi,[7] X. Liu,[3] D. Loh,[50] A. Loi,[16] I. Longstaff,[53] J. H. Lopes,[2] D. Lucchesi,[23,q] M. Lucio Martinez,[39] H. Luo,[52] A. Lupato,[23] E. Luppi,[17,a] O. Lupton,[40] A. Lusiani,[24] X. Lyu,[63] F. Machefert,[7] F. Maciuc,[30] V. Macko,[41] P. Mackowiak,[10] S. Maddrell-Mander,[48] O. Maev,[31,40] K. Maguire,[56] D. Maisuzenko,[31] M. W. Majewski,[28] S. Malde,[57] B. Malecki,[27] A. Malinin,[68] T. Maltsev,[36,f] G. Manca,[16,g] G. Mancinelli,[6] D. Marangotto,[22,m] J. Maratas,[5,r] J. F. Marchand,[4] U. Marconi,[15] C. Marin Benito,[38] M. Marinangeli,[41]

P. Marino,[41] J. Marks,[12] G. Martellotti,[26] M. Martin,[6] M. Martinelli,[41] D. Martinez Santos,[39] F. Martinez Vidal,[71] A. Massafferri,[1] R. Matev,[40] A. Mathad,[50] Z. Mathe,[40] C. Matteuzzi,[21] A. Mauri,[42] E. Maurice,[7,c] B. Maurin,[41] A. Mazurov,[47] M. McCann,[55,40] A. McNab,[56] R. McNulty,[13] J. V. Mead,[54] B. Meadows,[59] C. Meaux,[6] F. Meier,[10] N. Meinert,[67] D. Melnychuk,[29] M. Merk,[43] A. Merli,[22,40,m] E. Michielin,[23] D. A. Milanes,[66] E. Millard,[50] M.-N. Minard,[4] L. Minzoni,[17] D. S. Mitzel,[12] A. Mogini,[8] J. Molina Rodriguez,[1] T. Mombächer,[10] I. A. Monroy,[66] S. Monteil,[5] M. Morandin,[23] M. J. Morello,[24,k] O. Morgunova,[68] J. Moron,[28] A. B. Morris,[52] R. Mountain,[61] F. Muheim,[52] M. Mulder,[43] D. Müller,[56] J. Müller,[10] K. Müller,[42] V. Müller,[10] P. Naik,[48] T. Nakada,[41] R. Nandakumar,[51] A. Nandi,[57] I. Nasteva,[2] M. Needham,[52] N. Neri,[22,40] S. Neubert,[12] N. Neufeld,[40] M. Neuner,[12] T. D. Nguyen,[41] C. Nguyen-Mau,[41,s] S. Nieswand,[9] R. Niet,[10] N. Nikitin,[33] T. Nikodem,[12] A. Nogay,[68] D. P. O'Hanlon,[50] A. Oblakowska-Mucha,[28] V. Obraztsov,[37] S. Ogilvy,[19] R. Oldeman,[16,g] C. J. G. Onderwater,[72] A. Ossowska,[27] J. M. Otalora Goicochea,[2] P. Owen,[42] A. Oyanguren,[71] P. R. Pais,[41] A. Palano,[14] M. Palutan,[19,40] A. Papanestis,[51] M. Pappagallo,[52] L. L. Pappalardo,[17,a] W. Parker,[60] C. Parkes,[56] G. Passaleva,[18,40] A. Pastore,[14,l] M. Patel,[55] C. Patrignani,[15,h] A. Pellegrino,[43] G. Penso,[26] M. Pepe Altarelli,[40] S. Perazzini,[40] D. Pereima,[32] P. Perret,[5] L. Pescatore,[41] K. Petridis,[48] A. Petrolini,[20,j] A. Petrov,[68] M. Petruzzo,[22,m] E. Picatoste Olloqui,[38] B. Pietrzyk,[4] G. Pietrzyk,[41] M. Pikies,[27] D. Pinci,[26] F. Pisani,[40] A. Pistone,[20,j] A. Piucci,[12] V. Placinta,[30] S. Playfer,[52] M. Plo Casasus,[39] F. Polci,[8] M. Poli Lener,[19] A. Poluektov,[50] I. Polyakov,[61] E. Polycarpo,[2] G. J. Pomery,[48] S. Ponce,[40] A. Popov,[37] D. Popov,[11,40] S. Poslavskii,[37] C. Potterat,[2] E. Price,[48] J. Prisciandaro,[39] C. Prouve,[48] V. Pugatch,[46] A. Puig Navarro,[42] H. Pullen,[57] G. Punzi,[24,t] W. Qian,[50] J. Qin,[63] R. Quagliani,[8] B. Quintana,[5] B. Rachwal,[28] J. H. Rademacker,[48] M. Rama,[24] M. Ramos Pernas,[39] M. S. Rangel,[2] I. Raniuk,[45,†] F. Ratnikov,[35,u] G. Raven,[44] M. Ravonel Salzgeber,[40] M. Reboud,[4] F. Redi,[41] S. Reichert,[10] A. C. dos Reis,[1] C. Remon Alepuz,[71] V. Renaudin,[7] S. Ricciardi,[51] S. Richards,[48] M. Rihl,[40] K. Rinnert,[54] P. Robbe,[7] A. Robert,[8] A. B. Rodrigues,[41] E. Rodrigues,[59] J. A. Rodriguez Lopez,[66] A. Rogozhnikov,[35] S. Roiser,[40] A. Rollings,[57] V. Romanovskiy,[37] A. Romero Vidal,[39,40] M. Rotondo,[19] M. S. Rudolph,[61] T. Ruf,[40] P. Ruiz Valls,[71] J. Ruiz Vidal,[71] J. J. Saborido Silva,[39] E. Sadykhov,[32] N. Sagidova,[31] B. Saitta,[16,g] V. Salustino Guimaraes,[62] C. Sanchez Mayordomo,[71] B. Sanmartin Sedes,[39] R. Santacesaria,[26] C. Santamarina Rios,[39] M. Santimaria,[19] E. Santovetti,[25,i] G. Sarpis,[56] A. Sarti,[19,v] C. Satriano,[26,w] A. Satta,[25] D. M. Saunders,[48] D. Savrina,[32,33] S. Schael,[9] M. Schellenberg,[10] M. Schiller,[53] H. Schindler,[40] M. Schmelling,[11] T. Schmelzer,[10] B. Schmidt,[40] O. Schneider,[41] A. Schopper,[40] H. F. Schreiner,[59] M. Schubiger,[41] M. H. Schune,[7] R. Schwemmer,[40] B. Sciascia,[19] A. Sciubba,[26,v] A. Semennikov,[32] E. S. Sepulveda,[8] A. Sergi,[47] N. Serra,[42] J. Serrano,[6] L. Sestini,[23] P. Seyfert,[40] M. Shapkin,[37] I. Shapoval,[45] Y. Shcheglov,[31] T. Shears,[54] L. Shekhtman,[36,f] V. Shevchenko,[68] B. G. Siddi,[17] R. Silva Coutinho,[42] L. Silva de Oliveira,[2] G. Simi,[23,q] S. Simone,[14,l] M. Sirendi,[49] N. Skidmore,[48] T. Skwarnicki,[61] I. T. Smith,[52] J. Smith,[49] M. Smith,[55] l. Soares Lavra,[1] M. D. Sokoloff,[59] F. J. P. Soler,[53] B. Souza De Paula,[2] B. Spaan,[10] P. Spradlin,[53] S. Sridharan,[40] F. Stagni,[40] M. Stahl,[12] S. Stahl,[40] P. Stefko,[41] S. Stefkova,[55] O. Steinkamp,[42] S. Stemmle,[12] O. Stenyakin,[37] M. Stepanova,[31] H. Stevens,[10] S. Stone,[61] B. Storaci,[42] S. Stracka,[24,t] M. E. Stramaglia,[41] M. Straticiuc,[30] U. Straumann,[42] J. Sun,[3] L. Sun,[64] K. Swientek,[28] V. Syropoulos,[44] T. Szumlak,[28] M. Szymanski,[63] S. T'Jampens,[4] A. Tayduganov,[6] T. Tekampe,[10] G. Tellarini,[17,a] F. Teubert,[40] E. Thomas,[40] J. van Tilburg,[43] M. J. Tilley,[55] V. Tisserand,[5] M. Tobin,[41] S. Tolk,[49] L. Tomassetti,[17,a] D. Tonelli,[24] R. Tourinho Jadallah Aoude,[1] E. Tournefier,[4] M. Traill,[53] M. T. Tran,[41] M. Tresch,[42] A. Trisovic,[49] A. Tsaregorodtsev,[6] P. Tsopelas,[43] A. Tully,[49] N. Tuning,[43,40] A. Ukleja,[29] A. Usachov,[7] A. Ustyuzhanin,[35] U. Uwer,[12] C. Vacca,[16,g] A. Vagner,[70] V. Vagnoni,[15,40] A. Valassi,[40] S. Valat,[40] G. Valenti,[15] R. Vazquez Gomez,[40] P. Vazquez Regueiro,[39] S. Vecchi,[17] M. van Veghel,[43] J. J. Velthuis,[48] M. Veltri,[18,x] G. Veneziano,[57] A. Venkateswaran,[61] T. A. Verlage,[9] M. Vernet,[5] M. Vesterinen,[57] J. V. Viana Barbosa,[40] D. Vieira,[63] M. Vieites Diaz,[39] H. Viemann,[67] X. Vilasis-Cardona,[38,b] M. Vitti,[49] V. Volkov,[33] A. Vollhardt,[42] B. Voneki,[40] A. Vorobyev,[31] V. Vorobyev,[36,f] C. Voß,[9] J. A. de Vries,[43] C. Vázquez Sierra,[43] R. Waldi,[67] J. Walsh,[24] J. Wang,[61] Y. Wang,[65] D. R. Ward,[49] H. M. Wark,[54] N. K. Watson,[47] D. Websdale,[55] A. Weiden,[42] C. Weisser,[58] M. Whitehead,[40] J. Wicht,[50] G. Wilkinson,[57] M. Wilkinson,[61] M. Williams,[56] M. Williams,[58] T. Williams,[47] F. F. Wilson,[51,40] J. Wimberley,[60] M. Winn,[7] J. Wishahi,[10] W. Wislicki,[29] M. Witek,[27] G. Wormser,[7] S. A. Wotton,[49] K. Wyllie,[40] Y. Xie,[65] M. Xu,[65] Q. Xu,[63] Z. Xu,[3] Z. Xu,[4] Z. Yang,[3] Z. Yang,[60] Y. Yao,[61] H. Yin,[65] J. Yu,[65] X. Yuan,[61] O. Yushchenko,[37] K. A. Zarebski,[47] M. Zavertyaev,[11,y] L. Zhang,[3] Y. Zhang,[7] A. Zhelezov,[12] Y. Zheng,[63] X. Zhu,[3] V. Zhukov,[9,33] J. B. Zonneveld,[52] and S. Zucchelli[15]

(LHCb Collaboration)

[1]*Centro Brasileiro de Pesquisas Físicas (CBPF), Rio de Janeiro, Brazil*
[2]*Universidade Federal do Rio de Janeiro (UFRJ), Rio de Janeiro, Brazil*
[3]*Center for High Energy Physics, Tsinghua University, Beijing, China*
[4]*Univ. Grenoble Alpes, Univ. Savoie Mont Blanc, CNRS, IN2P3-LAPP, Annecy, France*
[5]*Clermont Université, Université Blaise Pascal, CNRS/IN2P3, LPC, Clermont-Ferrand, France*
[6]*Aix Marseille Univ, CNRS/IN2P3, CPPM, Marseille, France*
[7]*LAL, Univ. Paris-Sud, CNRS/IN2P3, Université Paris-Saclay, Orsay, France*
[8]*LPNHE, Université Pierre et Marie Curie, Université Paris Diderot, CNRS/IN2P3, Paris, France*
[9]*I. Physikalisches Institut, RWTH Aachen University, Aachen, Germany*
[10]*Fakultät Physik, Technische Universität Dortmund, Dortmund, Germany*
[11]*Max-Planck-Institut für Kernphysik (MPIK), Heidelberg, Germany*
[12]*Physikalisches Institut, Ruprecht-Karls-Universität Heidelberg, Heidelberg, Germany*
[13]*School of Physics, University College Dublin, Dublin, Ireland*
[14]*Sezione INFN di Bari, Bari, Italy*
[15]*Sezione INFN di Bologna, Bologna, Italy*
[16]*Sezione INFN di Cagliari, Cagliari, Italy*
[17]*Universita e INFN, Ferrara, Ferrara, Italy*
[18]*Sezione INFN di Firenze, Firenze, Italy*
[19]*Laboratori Nazionali dell'INFN di Frascati, Frascati, Italy*
[20]*Sezione INFN di Genova, Genova, Italy*
[21]*Sezione INFN di Milano Bicocca, Milano, Italy*
[22]*Sezione di Milano, Milano, Italy*
[23]*Sezione INFN di Padova, Padova, Italy*
[24]*Sezione INFN di Pisa, Pisa, Italy*
[25]*Sezione INFN di Roma Tor Vergata, Roma, Italy*
[26]*Sezione INFN di Roma La Sapienza, Roma, Italy*
[27]*Henryk Niewodniczanski Institute of Nuclear Physics Polish Academy of Sciences, Kraków, Poland*
[28]*AGH–University of Science and Technology, Faculty of Physics and Applied Computer Science, Kraków, Poland*
[29]*National Center for Nuclear Research (NCBJ), Warsaw, Poland*
[30]*Horia Hulubei National Institute of Physics and Nuclear Engineering, Bucharest-Magurele, Romania*
[31]*Petersburg Nuclear Physics Institute (PNPI), Gatchina, Russia*
[32]*Institute of Theoretical and Experimental Physics (ITEP), Moscow, Russia*
[33]*Institute of Nuclear Physics, Moscow State University (SINP MSU), Moscow, Russia*
[34]*Institute for Nuclear Research of the Russian Academy of Sciences (INR RAS), Moscow, Russia*
[35]*Yandex School of Data Analysis, Moscow, Russia*
[36]*Budker Institute of Nuclear Physics (SB RAS), Novosibirsk, Russia*
[37]*Institute for High Energy Physics (IHEP), Protvino, Russia*
[38]*ICCUB, Universitat de Barcelona, Barcelona, Spain*
[39]*Instituto Galego de Física de Altas Enerxías (IGFAE), Universidade de Santiago de Compostela, Santiago de Compostela, Spain*
[40]*European Organization for Nuclear Research (CERN), Geneva, Switzerland*
[41]*Institute of Physics, Ecole Polytechnique Fédérale de Lausanne (EPFL), Lausanne, Switzerland*
[42]*Physik-Institut, Universität Zürich, Zürich, Switzerland*
[43]*Nikhef National Institute for Subatomic Physics, Amsterdam, The Netherlands*
[44]*Nikhef National Institute for Subatomic Physics and VU University Amsterdam, Amsterdam, The Netherlands*
[45]*NSC Kharkiv Institute of Physics and Technology (NSC KIPT), Kharkiv, Ukraine*
[46]*Institute for Nuclear Research of the National Academy of Sciences (KINR), Kyiv, Ukraine*
[47]*University of Birmingham, Birmingham, United Kingdom*
[48]*H. H. Wills Physics Laboratory, University of Bristol, Bristol, United Kingdom*
[49]*Cavendish Laboratory, University of Cambridge, Cambridge, United Kingdom*
[50]*Department of Physics, University of Warwick, Coventry, United Kingdom*
[51]*STFC Rutherford Appleton Laboratory, Didcot, United Kingdom*
[52]*School of Physics and Astronomy, University of Edinburgh, Edinburgh, United Kingdom*
[53]*School of Physics and Astronomy, University of Glasgow, Glasgow, United Kingdom*
[54]*Oliver Lodge Laboratory, University of Liverpool, Liverpool, United Kingdom*
[55]*Imperial College London, London, United Kingdom*
[56]*School of Physics and Astronomy, University of Manchester, Manchester, United Kingdom*
[57]*Department of Physics, University of Oxford, Oxford, United Kingdom*

[58]*Massachusetts Institute of Technology, Cambridge, MA, USA*
[59]*University of Cincinnati, Cincinnati, OH, USA*
[60]*University of Maryland, College Park, MD, USA*
[61]*Syracuse University, Syracuse, NY, USA*
[62]*Pontifícia Universidade Católica do Rio de Janeiro (PUC-Rio), Rio de Janeiro, Brazil (associated with Universidade Federal do Rio de Janeiro (UFRJ), Rio de Janeiro, Brazil)*
[63]*University of Chinese Academy of Sciences, Beijing, China (associated with Center for High Energy Physics, Tsinghua University, Beijing, China)*
[64]*School of Physics and Technology, Wuhan University, Wuhan, China (associated with Center for High Energy Physics, Tsinghua University, Beijing, China)*
[65]*Institute of Particle Physics, Central China Normal University, Wuhan, Hubei, China (associated with Center for High Energy Physics, Tsinghua University, Beijing, China)*
[66]*Departamento de Fisica, Universidad Nacional de Colombia, Bogota, Colombia (associated with LPNHE, Université Pierre et Marie Curie, Université Paris Diderot, CNRS/IN2P3, Paris, France)*
[67]*Institut für Physik, Universität Rostock, Rostock, Germany (associated with Physikalisches Institut, Ruprecht-Karls-Universität Heidelberg, Heidelberg, Germany)*
[68]*National Research Centre Kurchatov Institute, Moscow, Russia (associated with Institute of Theoretical and Experimental Physics (ITEP), Moscow, Russia)*
[69]*National University of Science and Technology MISIS, Moscow, Russia (associated with Institute of Theoretical and Experimental Physics (ITEP), Moscow, Russia)*
[70]*National Research Tomsk Polytechnic University, Tomsk, Russia (associated with Institute of Theoretical and Experimental Physics (ITEP), Moscow, Russia)*
[71]*Instituto de Fisica Corpuscular, Centro Mixto Universidad de Valencia–CSIC, Valencia, Spain (associated with ICCUB, Universitat de Barcelona, Barcelona, Spain)*
[72]*Van Swinderen Institute, University of Groningen, Groningen, The Netherlands (associated with Nikhef National Institute for Subatomic Physics, Amsterdam, The Netherlands)*
[73]*Los Alamos National Laboratory (LANL), Los Alamos, USA (associated with Syracuse University, Syracuse, NY, USA)*

[†]Deceased.
[a]Also at Università di Ferrara, Ferrara, Italy.
[b]Also at LIFAELS, La Salle, Universitat Ramon Llull, Barcelona, Spain.
[c]Also at Laboratoire Leprince-Ringuet, Palaiseau, France.
[d]Also at Università di Milano Bicocca, Milano, Italy.
[e]Also at Università di Modena e Reggio Emilia, Modena, Italy.
[f]Also at Novosibirsk State University, Novosibirsk, Russia.
[g]Also at Università di Cagliari, Cagliari, Italy.
[h]Also at Università di Bologna, Bologna, Italy.
[i]Also at Università di Roma Tor Vergata, Roma, Italy.
[j]Also at Università di Genova, Genova, Italy.
[k]Also at Scuola Normale Superiore, Pisa, Italy.
[l]Also at Università di Bari, Bari, Italy.
[m]Also at Università degli Studi di Milano, Milano, Italy.
[n]Also at National University of Science and Technology MISIS, Moscow, Russia.
[o]Also at Universidade Federal do Triângulo Mineiro (UFTM), Uberaba-MG, Brazil.
[p]Also at AGH–University of Science and Technology, Faculty of Computer Science, Electronics and Telecommunications, Kraków, Poland.
[q]Also at Università di Padova, Padova, Italy.
[r]Also at Iligan Institute of Technology (IIT), Iligan, Philippines.
[s]Also at Hanoi University of Science, Hanoi, Vietnam.
[t]Also at Università di Pisa, Pisa, Italy.
[u]Also at National Research University Higher School of Economics, Moscow, Russia.
[v]Also at Università di Roma La Sapienza, Roma, Italy.
[w]Also at Università della Basilicata, Potenza, Italy.
[x]Also at Università di Urbino, Urbino, Italy.
[y]Also at P. N. Lebedev Physical Institute, Russian Academy of Science (LPI RAS), Moscow, Russia.